American Mineralogist, Volume 82, pages 991–1000, 1997

Ferrous freudenbergite in ilmenite megacrysts: A unique paragenesis from the Dalnaya kimberlite, Yakutia

ALLAN D. PATCHEN,[1] LAWRENCE A. TAYLOR,[1] AND NIKOLAI POKHILENKO[2]

[1]Planetary Geosciences Institute, Department of Geological Sciences, The University of Tennessee, Knoxville, Tennessee 37996, U.S.A.
[2]Institute of Mineralogy and Petrography, Russian Academy of Science, Siberian Branch, Novosibirsk, Russia

ABSTRACT

A suite of picroilmenite megacrysts from the Dalnaya kimberlite, Siberia, was found to fall into one of two groups, the most abundant having 11–12 wt% MgO and 650–1500 ppm Nb, and the others having lower MgO (8.8–10.2 wt%) and higher Nb (1700–2700 ppm). Ferrous freudenbergite ($Na_2FeTi_7O_{16}$) crystals were found included in many of the megacrysts from the first group. The freudenbergite-bearing ilmenite megacrysts are also pervaded by micrometer-size spots that have elevated Al_2O_3 (>2 wt%), SiO_2 (>0.4 wt%), and Na_2O (>0.15 wt%) contents. The low Cr_2O_3 vs. Nb content of the second group may reflect clinopyroxene crystallization. This may be a factor influencing the lack of freudenbergite in these megacrysts.

All ferrous freudenbergite samples studied previously are manifested as metasomatic reaction mantles replacing rutile. The freudenbergite from the Dalnaya kimberlite described in this paper occurs as small (max. 150 μm × 40 μm), euhedral, prismatic inclusions in picroilmenite (11–12 wt% MgO) megacrysts, with no associated rutile. Minor-element (Cr, Al, and Mg) substitutions for Fe are more extensive than in previously studied freudenbergite, with up to 1.4 wt% Cr_2O_3, 1.9 wt% Al_2O_3, and 3.1 wt% MgO. Nb is relatively low, typically less than 0.3 wt% Nb_2O_5 with a maximum of 1.1 wt%. Reaction of some of the freudenbergite with an alkalic fluid has resulted in thin, discontinuous rims and embayments of perovskite and an unidentified hydrous calcium titanate, around most crystals. Rapid ascent from depth and shielding by ilmenite may have been contributing factors to the preservation of freudenbergite in these samples.

The significance of the euhedral nature of freudenbergite and the lack of any genetic relationship with rutile suggest that it crystallized by a process other than simple metasomatic replacement of rutile. Indeed, the freudenbergite probably crystallized directly from a Na + Ti-rich fluid infiltrating the ilmenite megacrysts. The several occurrences (Liberia, Bultfontein, and Dalnaya) of ferrous freudenbergite suggest that it may be more common in kimberlites than previously recognized.

INTRODUCTION

The type locality for the rare mineral freudenbergite is the apatite-rich Katzenbuckel (Odenwald, Germany) alkali-syenite complex, where it occurs as a xenomorphic accessory mineral associated with hematite (Frenzel 1961; Frenzel et al. 1971). Freudenbergite, sensu stricto $Na_2Fe^{3+}{}_2Ti_6O_{16}$, has only been observed in this complex. Ferrous analogs of freudenbergite ($Na_2FeTi_7O_{16}$) have been reported from xenoliths entrained in kimberlites. These were in lower crustal granulite xenoliths from Liberia (Haggerty 1983) and upper mantle zircon-bearing xenoliths with lindsleyite-mathiasite from Bultfontein, South Africa (Haggerty and Gurney 1984; Haggerty 1991). In the Liberian samples, ferrous freudenbergite occurs as the inner-most phase of reaction mantles on rutile, followed concentrically by ilmenite, perovskite, and sphene. This assemblage suggests that rutile reacted with an alkali-rich fluid, metasomatically precipitating freudenbergite first (Haggerty 1983). A sodium titanate, similar to freudenbergite in composition, was also observed mantling rutile in a kimberlite dike in the west Ukikit field, Yakutia (Oleinikov 1995). In the present study, the observed mineral occurs as small euhedral crystals embedded in picroilmenite megacrysts and, importantly, with no associated rutile or hematite.

Frenzel (1961) originally reported freudenbergite as hexagonal $Na_2Fe_2Ti_7O_{18}$, but McKie (1963) and McKie and Long (1970) corrected this to monoclinic $Na_2Fe_2Ti_6O_{16}$ on the the basis of observations of Wadsley (1964) that the X-ray data are similar to synthetic Na_xTiO_2 ''bronze.'' Bayer and Hoffman (1965) demonstrated extensive solid solution of the synthetic Na_xTiO_2 ''bronze,'' resulting in a general formula of $A_xB_yTi_{8-y}O_{16}$, where A = Na, Rb, and K; B = Fe, Mg, Al, Cr, Mn, Zn, Ni, Co,

0003–004X/97/0910–0991$05.00

TABLE 1. Average electron microprobe analyses of Dalnaya ilmenite megacrysts

Sample	315/84	251/84	367/79	370/84	114/84	393/84	377/84	331/84	243/84	4/84	304/84
*n**	34	36	35	34	50	36	37	36	42	36	35
Nb_2O_5	0.09(2)†	0.10(2)	0.12(2)	0.16(2)	0.17(1)	0.22(2)	0.10(2)	0.16(3)	0.28(2)	0.25(3)	0.39(4)
TiO_2	52.2(2)	52.2(4)	53.1(4)	52.2(4)	52.0(2)	51.7(5)	52.3(4)	52.6(2)	50.5(2)	47.7(3)	48.5(3)
ZrO_2	0.03(1)	<0.03	0.03(1)	0.03(1)	0.04(1)	0.04(1)	0.03(1)	0.03(1)	0.05(1)	0.06(1)	0.08(1)
Al_2O_3	0.67(9)	0.69(10)	0.59(6)	0.53(9)	0.58(5)	0.55(7)	0.66(9)	0.58(11)	0.53(4)	0.57(3)	0.49(7)
Cr_2O_3	1.44(2)	1.53(4)	0.83(2)	0.61(1)	0.56(1)	0.52(1)	1.37(6)	0.65(1)	1.03(2)	1.03(4)	0.72(2)
Fe_2O_3‡	7.63	7.46	7.07	7.86	7.94	8.49	7.81	7.32	9.47	13.9	12.5
FeO	25.7(2)	25.1(3)	25.7(9)	26.4(3)	27.2(2)	26.6(10)	24.5(4)	26.4(2)	27.2(1)	27.2(3)	27.9(2)
MgO	11.7(1)	12.1(2)	12.2(6)	11.4(1)	10.9(2)	11.1(7)	12.5(3)	11.6(2)	10.2(1)	8.73(15)	8.83(12)
MnO	0.23(1)	0.22(1)	0.25(3)	0.24(1)	0.27(1)	0.26(1)	0.23(1)	0.27(2)	0.28(1)	0.24(1)	0.30(2)
NiO	0.15(1)	0.17(1)	0.14(1)	0.11(1)	0.11(1)	0.10(1)	0.16(1)	0.12(1)	0.11(1)	0.10(1)	0.07(1)
Total	99.89	99.55	100.04	99.56	99.67	99.51	99.61	99.71	99.58	99.70	99.74
Cations on basis of three O atoms											
Nb	0.001	0.001	0.001	0.002	0.002	0.002	0.001	0.002	0.003	0.003	0.004
Ti	0.910	0.910	0.921	0.916	0.914	0.910	0.909	0.920	0.895	0.854	0.868
Zr	0.000	—	0.000	0.000	0.000	0.000	0.000	0.000	0.001	0.001	0.001
Al	0.018	0.019	0.016	0.015	0.016	0.015	0.018	0.016	0.015	0.016	0.014
Cr	0.026	0.028	0.015	0.011	0.011	0.010	0.025	0.012	0.019	0.019	0.014
Fe^{3+}	0.133	0.130	0.123	0.138	0.140	0.149	0.136	0.128	0.168	0.250	0.224
Fe^{2+}	0.499	0.486	0.496	0.515	0.531	0.520	0.473	0.514	0.535	0.542	0.556
Mg	0.406	0.418	0.420	0.396	0.380	0.387	0.431	0.402	0.358	0.310	0.313
Mn	0.005	0.005	0.005	0.005	0.005	0.005	0.004	0.005	0.006	0.005	0.006
Ni	0.003	0.003	0.003	0.002	0.002	0.002	0.003	0.002	0.002	0.002	0.001
Total	2.000	2.000	2.000	2.000	2.000	2.000	2.000	2.000	2.000	2.000	2.000
Ilm	51.4	50.2	50.7	52.6	54.1	53.0	48.7	52.4	54.8	55.5	56.7
Gk	41.8	43.1	43.0	40.4	38.7	39.4	44.3	41.0	36.6	31.7	31.9
Hem	6.9	6.7	6.3	7.0	7.1	7.6	7.0	6.5	8.6	12.8	11.4

* n = Number of analyses in average.
† Number in parentheses is 1 σ standard deviation in terms of the least unit cited.
‡ Fe_2O_3 calculated assuming ilmenite stoichiometry.

Cu, and Nb. Haggerty (1983) further simplified the formula to $A_2B_8O_{16}$, where A represents a large cation and B represents a smaller cation.

Experiments by Flower (1974) in the system Na_2O-Fe_2O_3-Al_2O_3-TiO_2-SiO_2 at 1000 bars pressure found that freudenbergite is stable over a range of temperatures (700–900 °C) and bulk compositions, at the Mn_2O_3-Mn_3O_4 f_{O_2} buffer. Although these conditions are consistent with the Katzenbuckel association, the freudenbergite observed in kimberlite xenoliths (Haggerty 1983; this study) probably formed at f_{O_2}closer to FMQ or WM. One set of experiments by Flower (1974) performed at an f_{O_2} of the Ni-NiO buffer resulted in the assemblage pyroxene + freudenbergite + ilmenite, indicating that freudenbergite is a stable mineral even under less oxidizing conditions.

The freudenbergite samples in this study are inclusions in ilmenite megacrysts collected from the Dalnaya kimberlite pipe, located in the Daldyn-Alakit region of western Yakutia, Siberia. Our collection of Dalnaya samples is dominated by picroilmenite and pyrope garnet megacrysts. Rodionov et al. (1990) suggested that xenoliths and megacrysts from Dalnaya may be products of deep-seated metasomatism of a mantle peridotite. The paragenesis of this occurrence of freudenbergite may be important to considerations of alkalis in kimberlite genesis.

ANALYTICAL METHODS

Small chips from 11 ilmenite megacrysts collected from the Dalnaya kimberlite pipe were mounted and polished for electron microprobe analysis. Freudenbergite was identified in six of these samples. One sample (315/84) was also mounted as an intact megacryst. Chemical analyses were performed with a CAMECA SX50 electron microprobe in the Department of Geological Sciences at the University of Tennessee. Digital backscattered electron (BSE) images and X-ray maps were acquired using an Oxford Instruments eXL-II Energy Dispersive Spectrometer (EDS) interfaced to the CAMECA SX50. Operating conditions for chemical analyses were 15 keV accelerating voltage, 20 nA beam current, and 1–5 μm beam diameter for freudenbergite and 15 keV, 30 nA, and 10 μm, respectively, for ilmenite. Peak counting times were 20 s for Fe and Ti, 30 s for Cr, Na, Mg, Si, and Al and 50 s for the remainder (Mn, Ni, Ca, Nb, Zr, and K). Standards were a combination of natural and synthetic compounds and pure elements. The CAMECA PAP (Pouchou and Pichoir 1985) correction procedure was applied to the instrumentally corrected data.

PETROGRAPHY

The Dalnaya kimberlite pipe is rich in titaniferous xenoliths and megacrysts (Rodionov et al. 1990). Besides the 11 ilmenite megacrysts, our collection includes garnet megacrysts consisting of titanian pyrope (20 wt% MgO, 0.6–1.1 wt% TiO_2) and a diopsidic pyroxene ($Wo_{45}En_{49}Fs_6$). The garnets are highly variable in Cr (1.4–8.9 wt% Cr_2O_3), with a range of Ca and Fe content (4.5–6.5 wt% CaO and 7.4–10.3 wt% FeO). All garnets plot

TABLE 2. Electron microprobe analyses of ilmenite megacryst textural features

Sample	315/84	315/84	114/79	114/79	315/84	114/79	243/84	4/84
feature	dot	normal	dot	normal	rim	rim	rim	rim
*n**	6	6	5	4	13	6	9	4
Nb_2O_5	0.11(3)†	0.12(1)	0.18(2)	0.18(3)	0.11(2)	0.17(2)	0.22(6)	0.27(3)
SiO_2	0.45(37)	<0.03	0.51(34)	<0.03	<0.03	<0.03	0.03(2)	<0.03
TiO_2	52.2(4)	52.5(1)	52.1(5)	52.3(1)	54.1(5)	53.9(7)	54.1(7)	49.7(3)
ZrO_2	<0.03	0.05(2)	0.03(3)	0.04(2)	0.04(2)	0.07(3)	0.06(2)	0.04(1)
Al_2O_3	2.10(40)	0.12(5)	2.58(38)	0.27(5)	0.63(20)	0.78(8)	0.81(9)	0.27(15)
Cr_2O_3	1.47(8)	1.42(4)	0.50(4)	0.54(2)	1.90(45)	0.92(19)	1.19(37)	1.14(1)
Fe_2O_3‡	7.44	8.02	6.69	7.72	5.72	7.82	7.38	13.3
FeO	23.8(5)	26.3(2)	24.3(10)	27.4(3)	22.2(5)	21.6(14)	21.0(25)	19.6(7)
MgO	12.6(3)	11.6(1)	12.4(7)	10.9(0)	14.5(3)	14.8(6)	15.3(5)	13.7(6)
CaO	0.03(2)	<0.03	0.04(3)	<0.03	0.08(5)	0.17(12)	0.15(10)	0.10(9)
MnO	0.21(3)	0.19(2)	0.27(1)	0.24(1)	0.42(6)	0.38(5)	0.43(6)	0.86(6)
NiO	0.15(1)	0.16(3)	0.11(2)	0.10(2)	0.12(3)	0.12(2)	0.13(2)	0.06(1)
Na_2O	0.19(17)	<0.03	0.18(16)	<0.03	<0.03	<0.03	<0.03	<0.03
Total	100.84	100.49	99.92	99.78	99.89	100.94	100.75	99.00
				Cations on basis of three O atoms				
Nb	0.001	0.001	0.002	0.002	0.001	0.002	0.002	0.003
Si	0.010	—	0.012	—	—	—	—	—
Ti	0.888	0.913	0.893	0.920	0.923	0.912	0.912	0.865
Zr	—	0.001	0.000	0.000	0.000	0.001	0.001	0.001
Al	0.056	0.003	0.069	0.008	0.017	0.021	0.021	0.007
Cr	0.026	0.026	0.009	0.010	0.034	0.016	0.021	0.021
Fe^{3+}	0.126	0.140	0.115	0.136	0.098	0.132	0.124	0.231
Fe^{2+}	0.451	0.509	0.463	0.536	0.421	0.406	0.393	0.380
Mg	0.425	0.399	0.421	0.381	0.492	0.496	0.510	0.471
Ca	0.001	—	0.001	—	0.002	0.004	0.004	0.002
Mn	0.004	0.004	0.005	0.005	0.008	0.007	0.008	0.017
Ni	0.003	0.003	0.002	0.002	0.003	0.002	0.002	0.001
Na	0.009	—	0.008	—	—	—	—	—
Total	2.000	2.000	2.000	2.000	2.000	2.000	2.000	2.000
Ilm	48.0	52.0	49.2	54.4	43.8	41.9	40.7	39.3
Gk	45.3	40.8	44.7	38.7	51.1	51.2	52.8	48.7
Hem	6.7	7.2	6.1	6.9	5.1	6.8	6.4	12.0

Note: Features "dot" and "normal" refer to mottled ilmenite megacryst texture.
* n = Number of analyses in average.
† Number in parentheses is 1 σ standard deviation in terms of the least unit cited.
‡ Fe_2O_3 calculated assuming ilmenite stoichiometry.

in the lherzolitic trend of Sobolev et al. (1973). The pyroxene-megacryst, non-quadrilateral components are 1.2 wt% Na_2O, 1.6% wt% Al_2O_3, 0.2 wt% Cr_2O_3, and 0.2 wt% TiO_2. The genetic relationship between the ilmenite megacrysts and the garnet and pyroxene megacrysts is presently unknown.

Ilmenite

Ilmenite megacrysts (1–2 cm) are rounded, dominantly single crystals, many containing aggregated areas of polycrystalline ilmenite. These areas consist of both polygonal and amoeboidal grains imparting a granoblastic texture to that portion of the megacryst. All ilmenite megacrysts contain thin (1–15 μm), higher-MgO ilmenite veinlets. These veinlets commonly contain small amounts of perovskite. Narrow (~50 μm), embayed rims are common where the megacryst is in contact with the kimberlite host. Except for these rims and veinlets, variations of all elements, with the exception of Al_2O_3, do not exceed counting statistics in each individual megacrysts (Table 1). The rims and veinlets are higher in MgO (14.5 vs. 11.7 wt%; Table 2, Figs. 1, 2a, and 2c), MnO (0.42 vs. 0.23 wt%; Table 2), and Cr_2O_3 (1.90 vs. 1.44 wt%; Table 2, Figs. 2a and 2c) compared with rest of the megacryst.

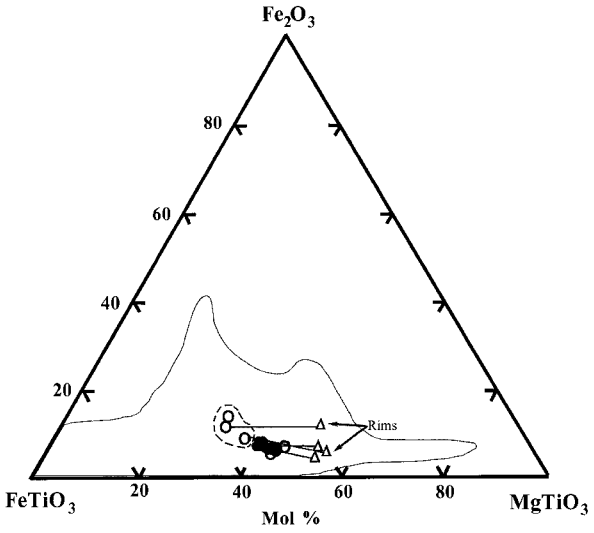

FIGURE 1. Hematite-ilmenite-geikielite plot of Dalnaya ilmenite megacryst compositions. Closed circles are freudenbergite-bearing megacrysts, open circles are megacrysts with no freudenbergite observed, and triangles are rim analyses. Dashed circle encloses three samples constituting freudenbergite-free group of megacrysts (see text).

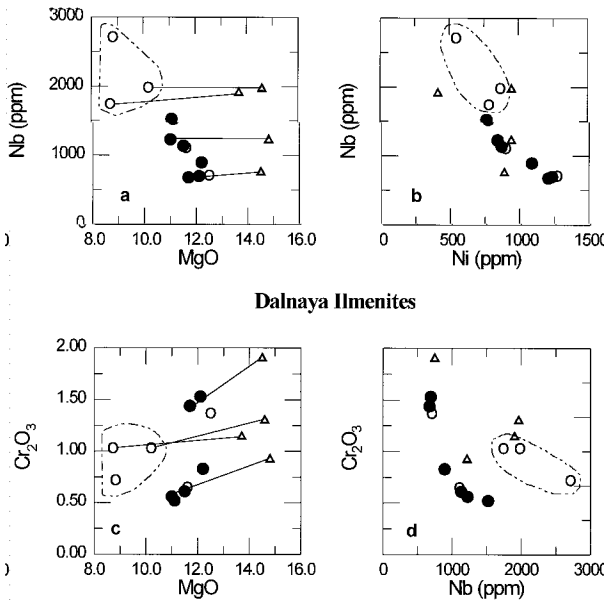

FIGURE 2. Element-element plots of Dalnaya ilmenite megacrysts. (**a**) Nb vs. MgO, (**b**) Nb vs. Ni, (**c**) Cr_2O_3 vs. MgO, (**d**) Cr_2O_3 vs. Nb. Symbols and dashed circles as in Figure 1.

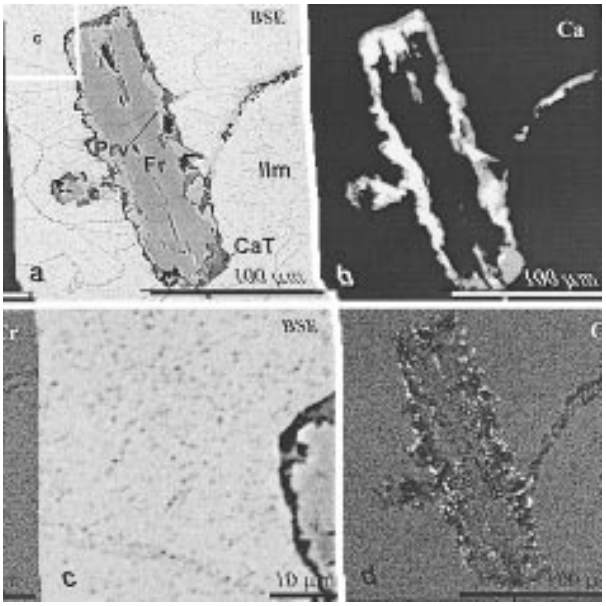

FIGURE 3. A BSE image (**a**), Ca X-ray map (**b**), and Cr X-ray map (**d**) of freudenbergite (Fr) in sample 315/84 Ilmenite (Ilm) megacryst. Ca-rich areas (**b**) are perovskite (Prv), intermediate Ca is an unidentified calcium titanate. Figure 3c is an enlargement of the area marked 'c' on the BSE image (**a**), showing the mottling in the ilmenite. Ca-rich areas (**d**) are residual spinels in the rim surrounding freudenbergite.

These ilmenite megacrysts span a range of compositions (Hem_6Gk_{43} to $Hem_{13}Gk_{32}$; Table 1, Fig. 1) similar to discrete ilmenite grains from other kimberlites (Haggerty 1989; 1991). MgO ranges from 8.7 wt% to 12.5 wt%, Cr_2O_3 from 0.5 to 1.5 wt%, and Nb_2O_5 from 0.07 to 0.4 wt% (Table 1). Trace- and major-element trends delineate at least two distinct populations of ilmenite megacrysts (Figs. 1 and 2a–d). The most abundant megacrysts sampled are those with 11–12 wt% MgO and 650–1500 ppm Nb. Three samples (243/84, 4/84, and 304/84) having lower MgO (8.8–10.2 wt%) and higher Nb (1700–2700 ppm) constitute the other group (Figs. 2a–d). The first group of megacrysts may be divided into Cr-poor and Cr-rich populations (<0.9 wt% and >1.3 wt% Cr_2O_3, respectively; Figs. 2c–d). This gap in composition may be an artifact of the population size.

Freudenbergite is observed only in the megacrysts with ilmenite having 11–12 wt% MgO and 650–1500 ppm Nb. An unusual textural feature of the freudenbergite-bearing ilmenite is that they are pervaded by micrometer size ''dots,'' which appear as a dark mottling in backscattered electron images (Fig. 3c) and are too small ($\leq$1 μm) for quantitative analysis. However, semi-quantitative analyses show elevated Al_2O_3 (up to 2.1 wt%), Na_2O (up to 0.19 wt%), and SiO_2 (up to 0.5 wt%) (Table 2 ''dots''). Adjacent normal ilmenite contains $\leq$0.3 wt% Al_2O_3, whereas Na_2O and SiO_2 are not detectable (<0.03 wt%) (Table 2 ''normal''). Note that the high-Mg ilmenite veinlets lack this mottling (Fig. 4). Average ilmenite analyses reported in Table 1 are defocused (10 μm) beam analyses and integrate both dots and normal ilmenite.

Although the focus of this study is freudenbergite, a summary of the paragenesis of the host picroilmenite megacrysts is essential. There is no absolute pressure or temperature that can be determined from these discrete ilmenite megacrysts. A source region for discrete picroilmenite megacrysts is generally assumed to be either the fertile lithosphere-asthenosphere boundary region, or a metasomatic zone at approximately 75–100 km depth (Haggerty 1989). Rodionov et al. (1990) suggested that the megacryst suite from Dalnaya has equilibrated at approximately 30 kbar and 900–1050 °C, consistent with a provenance from the metasomatic horizon. The hematite and geikielite components (Table 1, Fig. 1) of these ilmenite megacrysts are similar to discrete picroilmenite megacrysts from kimberlites (Haggerty 1989). For most megacrysts from other kimberlites, an f_{O_2} near the wustite-magnetite buffer has been suggested by Haggerty (1989; 1991) on the basis of the 1300 °C, 30 kbar, controlled f_{O_2} experiments by Woermann et al. (1970). The ilmenite megacrysts from Dalnaya probably formed under similar f_{O_2} conditions.

The smooth, linear correlation of MgO vs. Nb (Fig. 2a) and Ni vs. Nb (Fig. 2b) suggests that these ilmenite crystals may be the result of fractional crystallization of a mafic melt that may be a precursor to the kimberlite magma (Griffin et al. 1997). The presence of two compositionally distinct populations may be indicative of a change in the crystallizing mineral assemblage or influx of undifferentiated magma. Crystallization of clinopyrox-

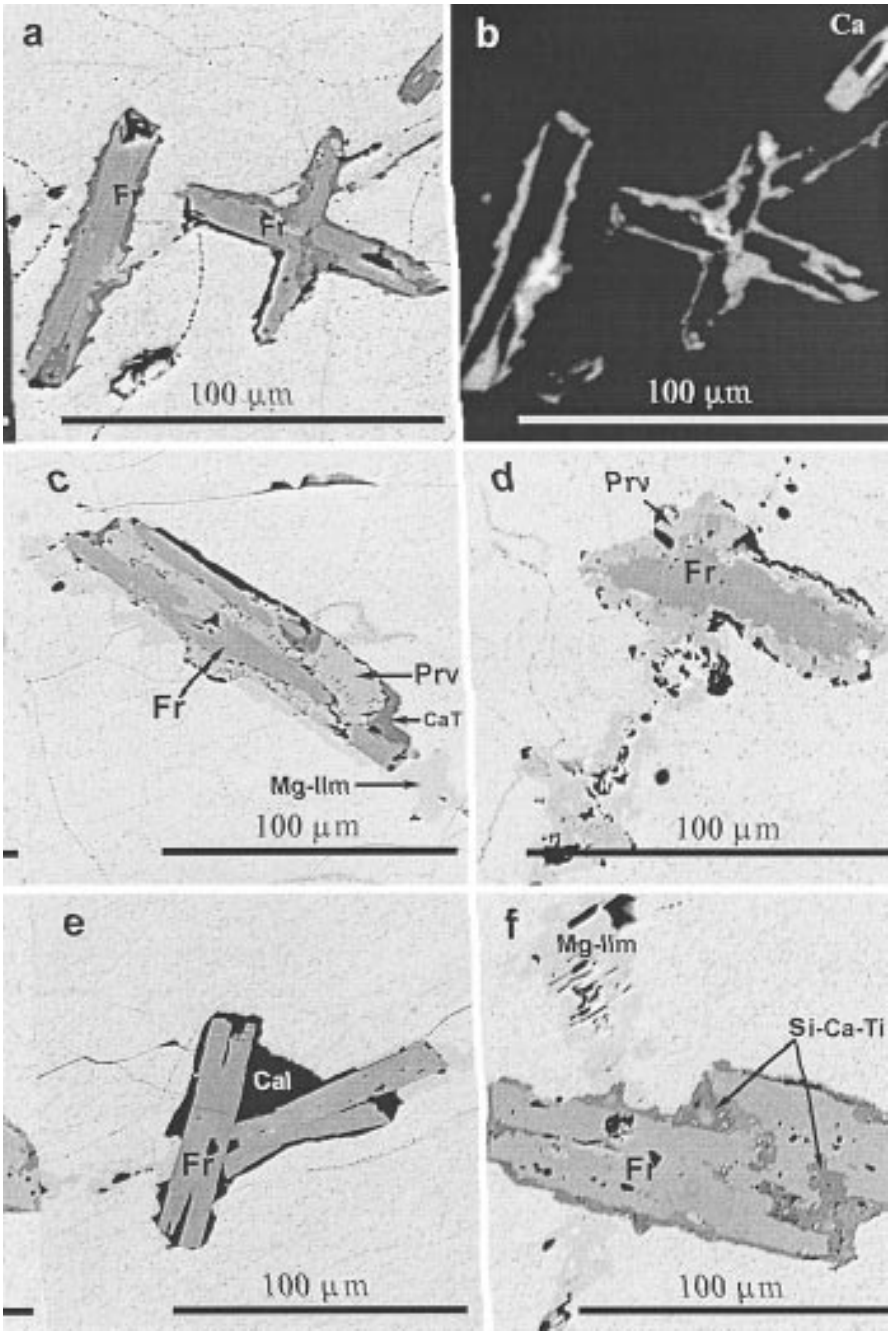

FIGURE 4. BSE images (**a, c–f**) and Ca X-ray map (**b**) of freudenbergite and associated phases. (**a**) and (**b**) show a penetration twin with hydrated calcium titanate rims (315/84). 4c (393/84) is a freudenbergite (Fr) with extensive perovskite (Prv) replacing it. Also present are hydrated Ca-Ti rims (CaT) and an ilmenite vein with higher MgO (Mg-Ilm). (**d**) is (114/79) freudenbergite (Fr) with perovskite (Prv) rims. (**e**) is (393/84), an unaltered freudenbergite with calcite (Cal). (**f**) is (315/84), which shows extensive hydrated Ca-Ti rims and patches of an also unidentified hydrated calcium and silicon titanate(s). Note also a wide vein of higher-MgO ilmenite (Mg-Ilm). In all BSE images, note pervasive mottling of the host ilmenite. Scale bar in all images is 100 μm.

ene may be indicated by the lower Cr_2O_3 content of the Nb-rich megacrysts (Fig. 2c) (Griffin et al. 1997). Lack of any discontinuity of the Ni vs. Nb curve (Fig. 2b) suggests that magma mixing was not a dominant process controlling the composition of these megacrysts (Griffin et al. 1997). The present data are insufficient to determine the evolution of the ilmenite crystallizing magma.

Either partial re-equilibration of ilmenite megacrysts with its host magma (Agee et al. 1982) or decreasing pressure (Haggerty et al. 1979) is evidenced by the ilmenite rims and veinlets richer in MgO. Alternatively, the increased Mg activity may have resulted from $MgCO_3$ metasomatism (Shulze et al. 1995).

The absence of exsolution or oxidation phases (e.g., spinel, rutile) in these megacrysts can be interpreted to indicate rapid eruption from depth, with effective quenching to below blocking temperatures. The elevated Al_2O_3 content of the dots in ilmenite may reflect incipient spinel exsolution. The inferred rapid ascent may also account for the preservation of freudenbergite.

Freudenbergite

The texture and composition of the freudenbergite of this study are unique. The ferrous freudenbergite from Dalnaya occurs as small (max. 150 μm × 40 μm), commonly twinned, prismatic crystals included in picroilmenite megacrysts (Figs. 3–5), whereas previously described occurrences are manifested as irregular reaction mantles on rutile (Haggerty 1983). In reflected light, freudenbergite has about the same reflectivity as perovskite, exhibits strong anisotropy, and commonly has thin (1–10 μm) alteration rims (Fig. 5). Under crossed polarizers, polysynthetic and penetration twinning is commonly observed. Freudenbergite crystals are occasionally found isolated in the ilmenite, but more commonly are associated with thin MgO-rich ilmenite veinlets and ilmenite subgrain boundaries. The long axes of freudenbergite crystals are generally oriented at a high angle to these boundaries and are fractured themselves occasionally. No preferred crystallographic orientation of the freudenbergite with the host ilmenite was observed. Both BSE and X-ray mapping (Figs. 3 and 4) reveal that the corroded margins of the freudenbergite crystals consist predominately of two phases, perovskite and an unidentified, possibly hydrated (low totals), calcium titanate (Table 3). The low analytical totals of these rims are not likely the consequence of small grain size, poor polish, or beam damage. Analysis of similar-sized perovskite rims result in good totals (Table 3). Beam damage was minimized by using a 10 nA beam current. A qualitative wavelength scan indicated an approximately 15% higher count rate for O in the hydrous rims than in the perovsikite rims, and no elements heavier than B, other than those reported, were detected. These rims are approximately the same width as the associated MgO-rich ilmenite veinlets and are commonly cuspate into both the ilmenite and freudenbergite (Figs. 3–5). Alteration penetrating into the freudenbergite crystals is almost entirely perovskite (Fig. 3b). The perovskite is nearly pure $CaTiO_3$ (Table 3), with only minor FeO (~3 wt%) and less than 0.02 wt% of Ce, La, and Na. In one freudenbergite crystal, in addition to the calcium titanates, there is an unidentified, hydrated (?), calcium titanium silicate (Table 3, Fig. 4f). Most crystals have partial to complete Ca-rich rims, but ilmenite megacrysts having the narrowest and lowest density

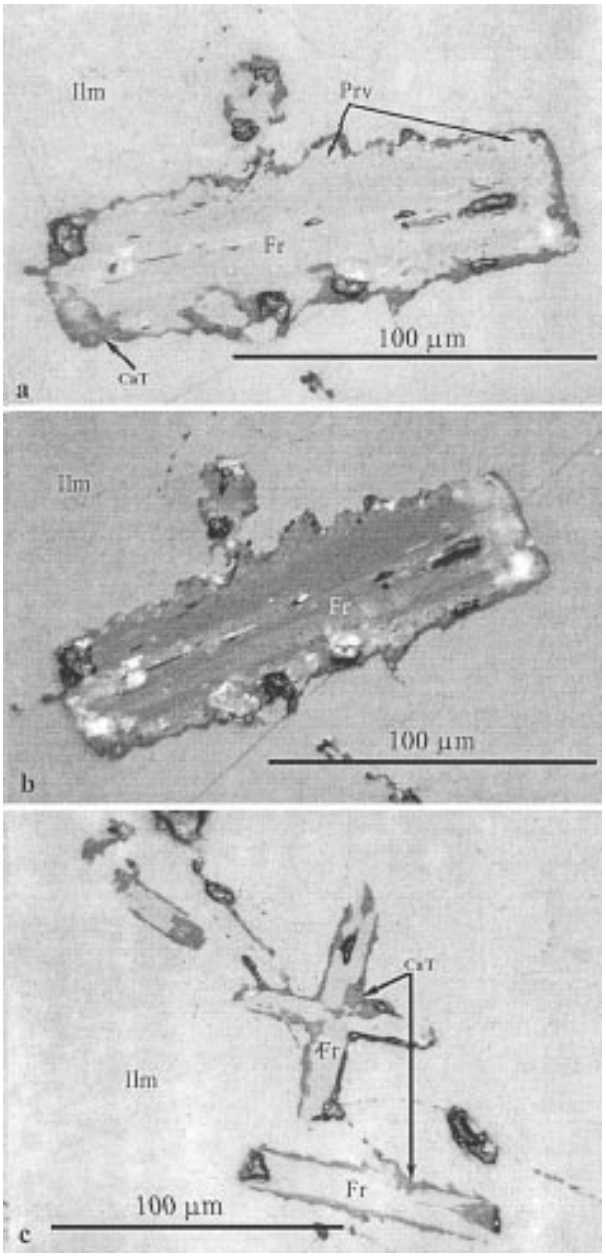

FIGURE 5. Oil immersion, reflected-light photomicrographs of freudenbergite in ilmenite. (**a**) (315/84) is same grain as Figures 3a–d. Dark areas surrounding freudenbergite crystal is a hydrated calcium titanate. (**b**) (crossed polarizers) showing twinning. (**c**) This is same grain as Figures 4a and 4b. Scale bar is 100 μm.

TABLE 3. Electron microprobe analyses of associated phases

Sample phase	315/84 Prv	393/84 Prv	315/84 CaT	315/84 CaT	393/84 CaT	393/84 CaT	315/84 CaSiT
Nb_2O_5	0.21	0.29	0.11	0.08	0.18	0.16	<0.03
SiO_2	0.15	<0.03	0.38	0.17	0.23	0.31	16.0
TiO_2	55.2	54.3	46.5	51.3	52.9	44.0	22.2
CeO_2	<0.03	<0.03	<0.03	<0.03	<0.03	<0.03	<0.03
Al_2O_3	<0.03	<0.03	1.21	0.89	2.06	0.85	0.34
Cr_2O_3	0.19	<0.03	2.90	1.70	0.85	0.69	0.42
La_2O_3	<0.03	<0.03	<0.03	<0.03	<0.03	<0.03	<0.03
MgO	<0.03	<0.03	4.61	3.15	3.71	4.19	0.07
CaO	40.5	40.7	22.4	22.8	23.6	23.9	37.6
MnO	<0.03	<0.03	0.54	0.88	0.12	0.07	0.10
FeO^t	2.76	3.75	7.23	6.72	3.07	10.0	12.2
NiO	<0.03	<0.03	<0.03	<0.03	<0.03	<0.03	<0.03
Na_2O	<0.03	<0.03	<0.03	<0.03	<0.03	<0.03	<0.03
Total	98.93	99.04	85.95	87.69	86.69	84.29	88.8
			Cations on basis of three O atoms				
Nb	0.002	0.003	0.001	0.001	0.002	0.002	—
Si	0.002	—	0.011	0.004	0.006	0.007	0.410
Ti	0.963	0.952	0.928	0.994	1.012	0.909	0.427
Ce	—	—	—	—	—	—	—
Al	0.000	0.000	0.038	0.027	0.062	0.028	0.010
Cr	0.004	0.000	0.061	0.035	0.017	0.015	0.009
La	—	—	—	—	—	—	—
Mg	0.000	0.000	0.182	0.121	0.141	0.172	0.002
Ca	1.008	1.015	0.638	0.631	0.642	0.704	1.032
Mn	0.000	0.000	0.012	0.019	0.002	0.002	0.002
Fe	0.054	0.073	0.160	0.145	0.065	0.232	0.262
Ni	0.000	0.000	0.000	0.000	0.000	0.000	0.000
Na	—	—	—	—	—	—	—
Total	2.034	2.043	2.031	1.973	1.950	2.069	2.153

Note: Prv = perovskite; CaT = hydrous(?) calcium titanate; CaSiT = hydrous(?) calcium silicon titanate.

of MgO-rich ilmenite veinlets have the best preserved freudenbergite crystals.

The TiO_2 and Na_2O in these freudenbergite crystals have similar compositional ranges (78.4–80.4 wt% and 8.0–8.7 wt%, respectively) as in other ferrous freudenbergite (Haggerty 1983, 1991), whereas FeO (5.5–7.5 wt%) is lower and more variable (Tables 4 and 5). Minor- and trace-element substitutions are significantly higher than in previously reported freudenbergite analysis (Frenzel 1961; McKie and Long 1970; Haggerty 1983, 1991), with the exception of Nb, which is usually less than 0.3 wt% Nb_2O_5, with a maximum of 1.1 wt% in this study (Tables 4 and 5; Fig. 6). Cr_2O_3 (0.6–1.9 wt%) is generally about the same as, or slightly higher than, the host picroilmenite (Tables 2 and 5). MgO (1.7–3.2 wt%) and Al_2O_3 (0.7–1.2 wt%) are the highest values yet reported for natural freudenbergite. All Fe is assumed to be Fe^{2+}, as suggested by the oxide and cation totals, and the assumed stoichiometry, making these freudenbergite crystals similar to the ferrous analog described by Haggerty (1983).

The freudenbergite samples from Dalnaya support the general formula of freudenbergite and extend the observed compositional variations. Previously reported as either $Na_2Fe^{3+}{}_2Ti_6O_{16}$ (McKie and Long 1970; Katzenbuckel) or $Na_2FeTi_7O_{16}$ (Haggerty 1983; Liberia), the primary difference is in the Fe^{3+} vs. Fe^{2+} content. The Katzenbuckel occurrence was an highly oxidizing environment, whereas the kimberlitic ones (Liberia and this study) appears to have been relatively less oxidizing. Therefore, it is reasonable to expect a trivalent-divalent cation substitution, coupled with Ti^{4+} content. Experimental work on Na_xTiO_2 ''bronze'' (Bayer and Hoffman 1965), relevant to freudenbergite, suggested that it could be represented as: $Na_xB^{2+}_yB^{3+}_zTi_{8-y-z}O_{16}$, where B^{2+} = Fe^{2+}, Mg, Ni, and Mn; B^{3+} = Fe^{3+}, Al, and Cr. Assuming that Nb is coupled with Ti, the data of Frenzel et al. (1971) closely match the trivalent end-member with $Na_{1.8}Fe^{3+}_{1.7}(Ti,Nb)_{6.25}O_{16}$, whereas the data of Haggerty (1983) could be related to the divalent end-member $Na_2(Fe^{2+},Mg)Ti_{6.93}O_{16}$ (Fig. 6). The Fe in the freudenbergite in this study is assumed to be entirely divalent, resulting in a formula with both trivalent and divalent cations, approximately $Na_{1.86}(Fe^{2+},Mg)_{1.1}(Cr,Al)_{0.25}Ti_{6.8}O_{16}$ (Tables 4 and 5).

FREUDENBERGITE PARAGENESIS

The morphology, association, and compositional range of freudenbergite from Dalnaya are unlike any previously described occurrences. These unique properties suggest a petrogenesis different from the metasomatic replacement of rutile (Haggerty 1983) or crystallization as an accessory mineral in an alkali syenite (Frenzel 1961). Below are discussed several possible models for their genesis.

Exsolution

The Dalnaya freudenbergite crystals are observed only as inclusions in ilmenite megacrysts. This raises the pos-

TABLE 4. Representative electron microprobe analyses of Dalnaya freudenbergites

Sample	315/84	315/84	315/84	251/84	114/79	367/84	370/84	393/84	393/84	393/84
Nb_2O_5	0.15	0.29	0.37	0.22	0.23	0.04	0.20	0.56	1.11	0.28
TiO_2	79.5	80.0	79.9	78.4	79.5	79.2	80.4	79.7	77.4	79.8
ZrO_2	0.04	<0.03	0.06	0.03	0.05	0.03	0.06	0.05	0.05	0.06
Al_2O_3	0.92	1.36	0.87	0.88	0.86	0.71	1.09	0.80	0.86	0.86
Cr_2O_3	1.43	1.64	0.65	1.92	0.56	0.89	0.66	0.47	0.92	0.50
MgO	1.68	2.41	3.16	2.45	2.70	2.80	2.42	2.48	1.45	2.54
CaO	0.30	0.13	0.43	0.30	0.63	0.22	0.93	0.71	0.52	0.73
MnO	<0.03	<0.03	<0.03	<0.03	<0.03	<0.03	<0.03	<0.03	<0.03	<0.03
FeO	7.50	5.83	5.53	7.40	6.56	6.95	5.97	6.66	8.99	6.58
NiO	0.09	0.06	0.07	0.05	0.03	0.04	<0.03	0.07	0.06	0.05
Na_2O	8.47	8.67	8.40	8.05	8.32	8.24	8.34	8.43	8.30	8.31
K_2O	<0.03	0.09	<0.03	0.15	<0.03	<0.03	<0.03	<0.03	<0.03	<0.03
Total	100.11	100.53	99.50	99.80	99.47	99.15	100.15	100.01	99.68	99.77
Cations on basis of 16 O atoms										
Nb	0.008	0.015	0.019	0.012	0.012	0.002	0.010	0.028	0.058	0.014
Ti	6.809	6.772	6.818	6.732	6.814	6.818	6.832	6.811	6.716	6.824
Zr	0.003	0.000	0.004	0.002	0.003	0.002	0.004	0.003	0.003	0.003
Al	0.123	0.181	0.117	0.119	0.116	0.096	0.145	0.108	0.116	0.116
Cr	0.128	0.146	0.058	0.173	0.050	0.080	0.059	0.042	0.084	0.045
Mg	0.286	0.404	0.535	0.417	0.548	0.477	0.407	0.420	0.250	0.431
Ca	0.036	0.015	0.052	0.036	0.078	0.027	0.112	0.086	0.064	0.090
Mn	—	—	—	—	—	—	—	—	—	—
Fe	0.714	0.549	0.525	0.707	0.626	0.666	0.564	0.633	0.868	0.625
Ni	0.008	0.005	0.007	0.004	0.003	0.004	0.001	0.006	0.006	0.005
Na	1.869	1.892	1.847	1.783	1.839	1.829	1.824	1.856	1.858	1.832
K	—	0.013	—	0.021	—	—	—	—	—	—
Total	9.986	9.994	9.986	10.006	10.004	10.005	9.962	9.997	10.026	9.988

sibility that these freudenbergite crystals formed by an exsolution process occurring in the ilmenite megacryst. Because there is no preferred crystallographic orientation with the host ilmenite, exsolution is considered to be an unlikely mechanism for freudenbergite formation. In addition, if they are the result of exsolution, one would expect to see a change in the density of Na-bearing dots in the host picroilmenite surrounding the freudenbergite, and this is not observed (Figs. 3 and 4).

Co-precipitation

Contemporaneous crystallization of the host picroilmenite megacryst and freudenbergite is suggested by the euhedral morphology of the freudenbergite crystals and compositional similarities (11–12 wt% MgO, 650–1500 ppm Nb) of the ilmenite grains they are included in. The similar Cr_2O_3 content of the host megacryst and included freudenbergite (Tables 1 and 5) suggests that they experienced at least partial attainment of equilibrium. Indeed, if the change of Cr_2O_3 composition in the MgO-poor, Nb-rich megacrysts is indicative of clinopyroxene crystallization (Griffin et al. 1997), the absence of freudenbergite in them may reflect a change in phase equilibria, perhaps with Na being preferentially partitioned into clinopyroxene. Additionally, the least altered and most abundant crystals of freudenbergite are found in those ilmenite megacrysts with the fewest MgO-rich ilmenite veinlets. This finding indicates both that the freudenbergite existed before the latest influx of fluids and that the survival of freudenbergite may depend upon being armored by ilmenite, thus isolated from resorption by the magma or other fluids. However, the association with veinlets and ilmenite subgrain boundaries, along with the previously described metasomatic replacement of rutile by ferrous freudenbergite (Haggerty 1983), casts doubt on a comagmatic origin of the freudenbergite and picroilmenite.

Metasomatism

All previously described occurrences of ferrous freudenbergite were the product of metasomatic replacement of rutile (Haggerty 1983, 1991), therefore a metasomatic origin for the Dalnaya freudenbergite must be considered. Most of the freudenbergite crystals from Dalnaya are associated with MgO-rich veinlets and ilmenite subgrain boundaries, common conduits for infiltrating fluids. This textural association strongly suggests that a metasomatic event influenced these samples. The absence of any relict rutile or replacement textures is problematic, but may be due to the complete replacement of rutile by freudenbergite. Rutile inclusions in ilmenite, having a similar morphology as the Dalnaya freudenbergite, were observed in the magnetite-free Snow Creek Anorthosite, part of the Laramie Anorthosite Complex, southeast Wyoming (D. Lindsley, personal communication). These rutile inclusions also have perovskite and calcium silicon titanate rims, but no freudenbergite. This assemblage may indicate a similar precursor phase in the Dalnaya megacrysts.

The perovskite and hydrous(?) calcium titanate alteration appears to be the result of secondary reaction of freudenbergite with an infiltrating Ca-rich fluid. The similarity in the widths of the veinlets and calcium titanate alteration rims on freudenbergite suggests that the fluid responsible for the formation of MgO-rich ilmenite postdates the crystallization of freudenbergite. If freudenbergite were the product of metasomatic replacement of ru-

TABLE 5. Average electron microprobe anlayses of Dalnaya freudenbergites

Sample	114/79	251/84	315/84	367/84	370/84	393/84
*n**	10	4	49	6	3	17
Nb_2O_5	0.23(12)†	0.18(4)	0.23(12)	0.20(11)	0.32(12)	0.40(20)
TiO_2	79.5(9)	78.8(5)	79.4(10)	79.5(8)	80.3(1)	79.7(9)
ZrO_2	0.05(1)	0.04(1)	0.04(2)	0.03(1)	0.07(2)	0.07(3)
Al_2O_3	0.86(15)	0.89(10)	1.04(38)	0.85(13)	1.03(5)	0.85(13)
Cr_2O_3	0.56(22)	1.74(32)	1.43(50)	1.03(19)	0.63(3)	0.65(21)
MgO	2.70(14)	2.22(48)	2.67(37)	2.56(29)	2.55(13)	2.38(29)
CaO	0.63(8)	0.22(12)	0.38(20)	0.21(12)	1.21(20)	0.71(21)
MnO	<0.03	<0.03	<0.03	<0.03	<0.03	<0.03
FeO	6.56(39)	8.16(95)	6.08(50)	6.74(54)	5.72(19)	6.47(50)
NiO	0.03(2)	0.02(1)	0.05(2)	0.05(1)	0.01(1)	0.04(2)
Na_2O	8.32(8)	8.29(22)	8.24(17)	8.20(11)	8.29(8)	8.34(18)
K_2O	<0.03	0.12(3)	<0.03	<0.03	<0.03	0.04(5)
Total	99.47	99.91	99.59	99.43	100.16	99.65
			Cations on basis of 16 O atoms			
Nb	0.012	0.009	0.012	0.010	0.017	0.021
Ti	6.814	6.719	6.787	6.820	6.818	6.823
Zr	0.003	0.002	0.002	0.001	0.004	0.004
Al	0.116	0.121	0.140	0.114	0.137	0.144
Cr	0.050	0.157	0.128	0.092	0.056	0.059
Mg	0.458	0.378	0.452	0.435	0.429	0.405
Ca	0.078	0.026	0.046	0.026	0.146	0.086
Mn	—	—	—	—	—	—
Fe	0.626	0.782	0.578	0.644	0.540	0.616
Ni	0.001	0.000	0.003	0.003	0.000	0.002
Na	1.839	1.840	1.815	1.813	1.815	1.841
K	—	0.023	—	—	—	0.007
Total	10.004	10.055	9.969	9.967	9.966	9.979

* n = Number of analyses in average.
† Number in parentheses is 1σ standard deviation in terms of the least unit cited.

tile, this alteration would require multiple metasomatic events interacting with these megacrysts. Alternatively, the freudenbergite may have formed by direct precipitation from a Na- and Ti-rich metasomatic fluid, with no intermediate phase (rutile) being replaced.

No other Na-bearing phases are intimately associated with the ilmenite megacrysts. The formation of perovskite appears to require removal from the megacryst of the Na from the reaction of freudenbergite and the fluid. Minor elements such as Cr and Al, that are incompatible in perovskite, remain in the alteration rims, as evidenced by high Cr spots within the reaction rims (Fig. 3c) and elevated Cr and Al in the hydrous (?) calcium titanate (Table 3). Mass balance would predict an increase of Na in the infiltrating fluid.

DISCUSSION

The upper mantle is generally accepted as the source region of kimberlitic melts. The high alkali, CO_2, and silicate incompatible-element contents of kimberlites, however, are not readily derived from only partial melting of an asthenospheric garnet lherzolite (Mitchell 1986). A possible source of these alkalis and incompatible elements is upper mantle metasomatism (Mitchell 1986; Wyllie 1989). Metasomatism preceding the main eruptive event, caused by volatile release of multiple aborted magma pulses, is one preferred model (Haggerty 1989). Intersection of the C-O-H peridotite solidus by protomelts may occur at two depths during assent, causing the release of metasomatic fluids (Wyllie 1989). The most like-

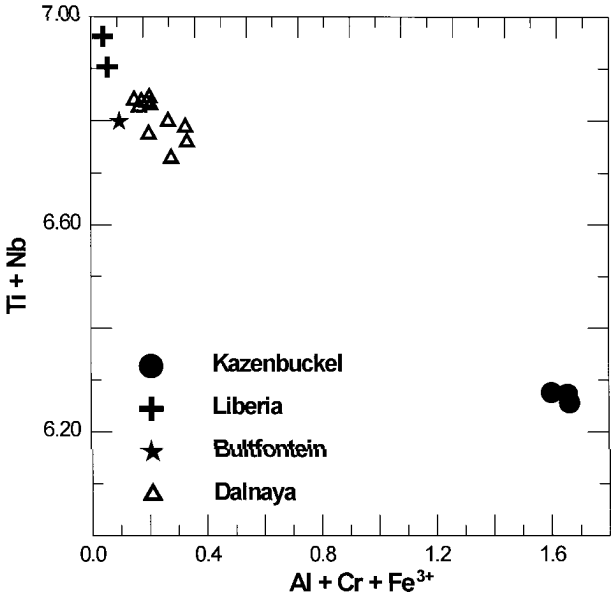

FIGURE 6. Plot of freudenbergite ΣB^{3+} vs. Ti and Nb from all known localities. Solid circles are those from Katzenbuckel (McKie and Long 1970; Frenzel et al. 1971) crosses are Liberian (Haggerty 1983), stars are from Bultfontein (Haggerty 1989), and triangles are from Dalnaya (this study).

ly is a metasomatic horizon at 60–100 km depths where melts intersect the thermal maximum of the C-O-H peridotite solidus (Wyllie 1989). This horizon may be divided into two zones, a lower K and H_2O dominated region and an upper Na and CO_2 dominated one (Haggerty 1989). The carbonate metasomatic zone is also relatively enriched in Ti + Nb + Zr + Fe (Haggerty 1989) A deeper level of metasomatism may occur near the lithosphere-asthenosphere boundary where the geotherm intersects the C-O-H peridotite solidus (Wyllie 1989).

Precipitation of freudenbergite may occur in the Na and CO_2 dominated metasomatic horizon, either by replacement of rutile or crystallization from a fluid. Interaction of freudenbergite with the C-O-H fluids, as the ilmenite megacryst moved upward and entered regions with higher Mg and Ca activity, leached Na from it and precipitate perovskite and other calcium titanates. This dissolution of freudenbergite may be another source of Na in the 60–100 km depth region. Freudenbergite is the only LIL titanate with significant concentrations of Na_2O (Haggerty 1991). Jadeitic omphacite in eclogites is the only other mantle mineral that has a level of Na similar to that of freudenbergite. It is possible that freudenbergite is present in the 60–100 km depth horizon and can contribute Na and high field strength elements to the generation of alkalic magmas.

Acknowledgments

This manuscript has been improved significantly by the comments and suggestions of Steve Haggerty and the thoughtful and effective reviews of D. Lindsley, D. Smith, and D. Mogk. A portion of this research was funded by NSF grants EAR93-04053 and EAR95-05930 to L.A.T., for which we are grateful.

References cited

Agee, J.J., Garrison, J.R., and Taylor, L.A. (1982) Petrogenesis of oxide minerals in kimberlite, Elliot County, Kentucky. American Mineralogist, 67, 28–42.

Bayer, G. and Hoffman, W. (1965) Uber Verbindugen vom Na_xTiO_2-Typ. Zeitschrift für Kristallographic, 121, 9–13.

Frenzel, G. (1961) Ein neues mineral: Freudenbergit ($Na_2Fe_2Ti_7O_{18}$). Nueus Jahrbuch für Mineralogie Monatshefte, 1961, 12–22.

Frenzel, G., Ottemann, J., and Nuber, B. (1971) Neue mikrosonden-untersuchungen an Freudenbergit. Nueus Jahrbuch für Mineralogie Monatshefte, 1971, 547–551.

Flower, M.J. (1974) Phase relations of titan-acmite in the system Na_2O-Fe_2O_3-Al_2O_3-TiO_2-SiO_2 at 1000 bars total water pressure. American Mineralogist, 59, 536–548.

Griffin, W.L., Moore, R.O., Ryan, C.G., Gurney, J.J., and Win, T.T. (1997) Geochemistry of magnesian ilmenite megacrysts from southern African kimberlites. Russian Geology and Geophysics, 38, No. 2, Proceeding of the Sixth International Kimberlite Conference, in press.

Haggerty, S.E. (1983) A freudenbergite-related mineral in granulites from Liberia. Nueus Jahrbuch für Mineralogie Monatshefte, 375–384.

——— (1989) Upper mantle opaque mineral stratigraphy and the genesis of metasomites and alkali-rich melts. in: Kimberlites and related rocks, vol. 2. Geological Society of Australia Special Publication no. 14, p. 687–699.

——— (1991) Oxide mineralogy of the upper mantle. In Mineralogical Society of America Reviews in Mineralogy, 25, 355–416.

Haggerty, S.E. and Gurney, J.J. (1984) Zircon-bearing nodules from the upper mantle. (abstract) EOS, 65, 301.

Haggerty, S.E., Hardie, R.B., and McMahon, B.M. (1979) The mineral chemistry of ilmenite nodule associations from the Monastery diatreme. In F.R. Boyd and H.O. Meyer, Eds., The Mantle Sample: Inclusions in kimberlites and other volcanics. Proceedings of the Second International Kimberlite Conference, vol. 2, p. 249–256. American Geophysical Union, Washington D.C.

McKie, D. (1963) The unit-cell of freudenbergite. Zeitschrift für Kristallographic, 119, 157–160.

McKie, D. and Long, J.V.P. (1970) The unit-cell contents of freudenbergite. Zeitschrift für Kristallographic, 132, 157–160.

Mitchell, R.H. (1986) Kimberlites: Mineralogy, Geochemistry, and Petrology. 442 p. Plenum Press, New York.

Oleinikov, O.B. (1995) Mineralogy of alkaline titanates-bearing kimberlite from a dike, West-Ukikit kimberlite field, Yakutia. Sixth International Kimberlite Conference extended abstracts, 404–405.

Pouchou, J.L. and Pichoir, F. (1985) ''PAP'' (phi-rho-Z) procedure for improved quantitative microanalysis. In J.T. Armstrong, Ed., Microbeam analysis, p. 104–108. San Francisco Press, San Francisco, California.

Rodionov, A.S., Sobolev, N.V., Pokhilenko, N.P., Suddaby, P., and Amshinsky, A.N. (1990) Ilmenite-bearing peridotites and megacrysts from Dalnaya kimberlite pipe, Yakutia. Fifth International Kimberlite Conference extended abstracts, 339–341.

Shulze, D.J., Anderson, P.F.N., Hearn, B.C., and Hetman, C.M. (1995) Origin and Significance of Ilmenite Megacrysts and Macrocrysts from kimberlite. International Geology Review, 37, 780–812.

Sobolev, N.V., Lavrentiev, Y.G., Pokhilenko, N.P., and Usova, L.V. (1973) Chrome-rich garnets from the kimberlites of Yakutia and their paragenesis. Contributions to Mineralogy and Petrology, 40, 39–52.

Wadsley, A.D. (1964) The possible identity of freudenbergite and Na_xTiO_2. Zeitschrift für Kristallographic, 120, 396–398.

Woermann, E., Hirschberg, A., and Lamprecht, A., (1970) Das system hematit-ilmenit-geikielith unter hohen temperatures und hohen druken. (abstract) Fortschrift fur Mineralogie 47, 79–80 (not seen; extracted from Mineralogical Society of America Reviews in Mineralogy, 25, 416, 1991.)

Wyllie, P.J. (1989) The genesis of kimberlites and some low-SiO_2, high-alkali magmas. In Kimberlites and related rocks vol. *2*, Geological Society of Australia Special Publication no. 14, 603–615.

Manuscript received July 15, 1996
Manuscript accepted May 8, 1997